# Henon-Heiles Hamiltonian (1964)

$$H = \frac{1}{2}\left(p_x^2 + p_y^2 + x^2 + y^2\right) + x^2 y - \frac{1}{3} y^3$$

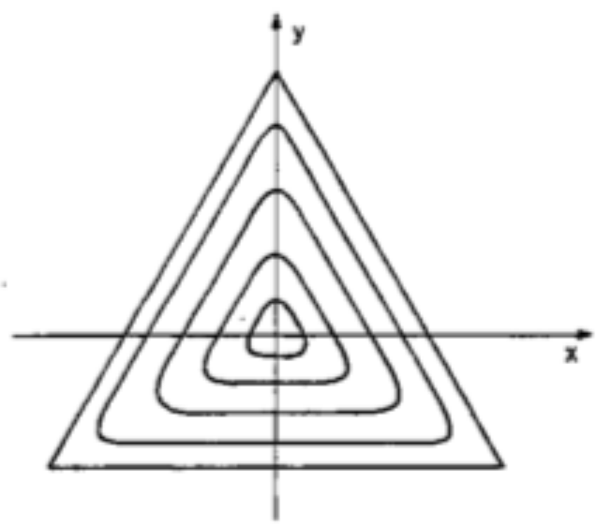


$$\begin{aligned} V(x,y) &= \frac{1}{2}\left(x^2 + y^2\right) + x^2 y - \frac{1}{3} y^3 \\ &= \frac{1}{2} r^2 + \frac{1}{3} r^3 \sin(3\theta) \end{aligned}$$

Motion is bounded up to *E=1/6*

# Integrate the equations of motion over time:

*E=1/8*

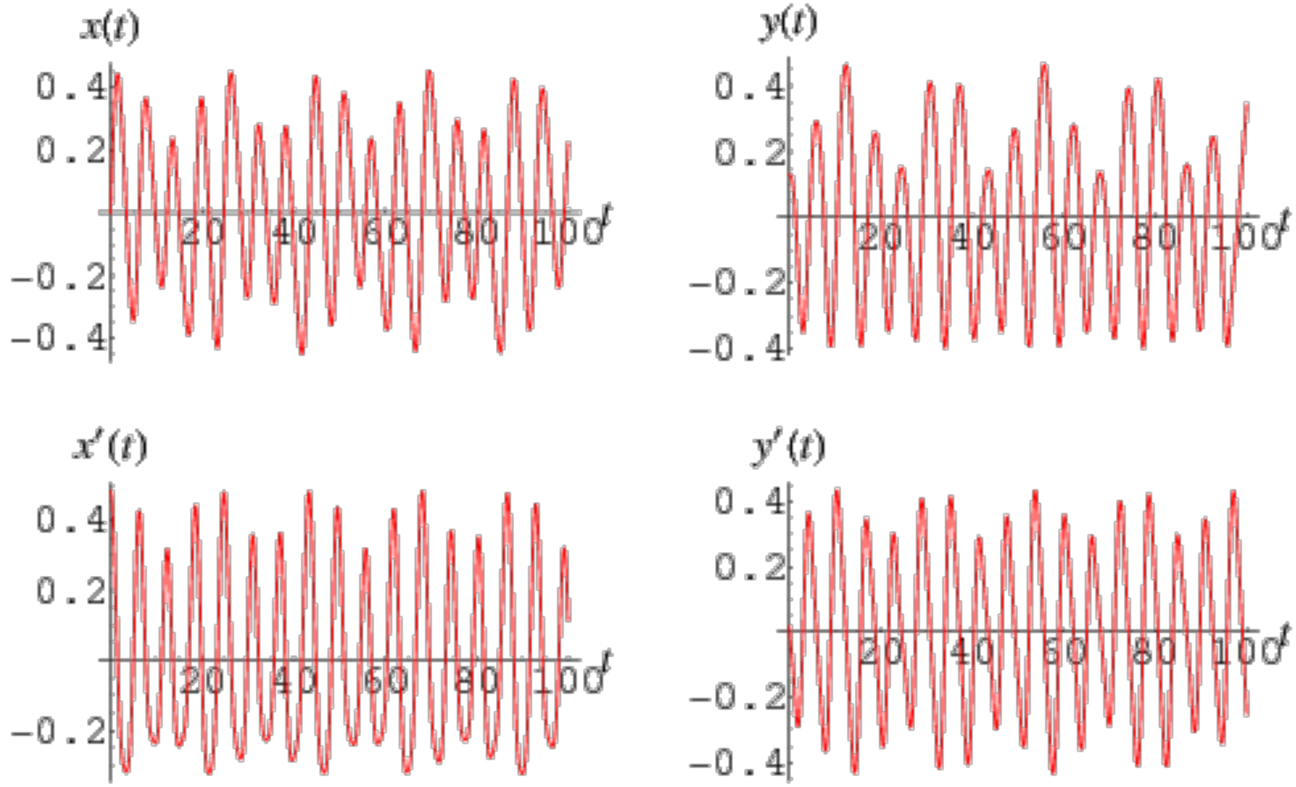


$$\dot{x} = \frac{\partial H}{\partial p_x} \qquad \dot{y} = \frac{\partial H}{\partial p_y}$$

$$\dot{p}_x = -\frac{\partial H}{\partial x} \qquad \dot{p}_y = -\frac{\partial H}{\partial y}$$

# Poincaré sections for the Henon-Heiles system

Henri Poincaré

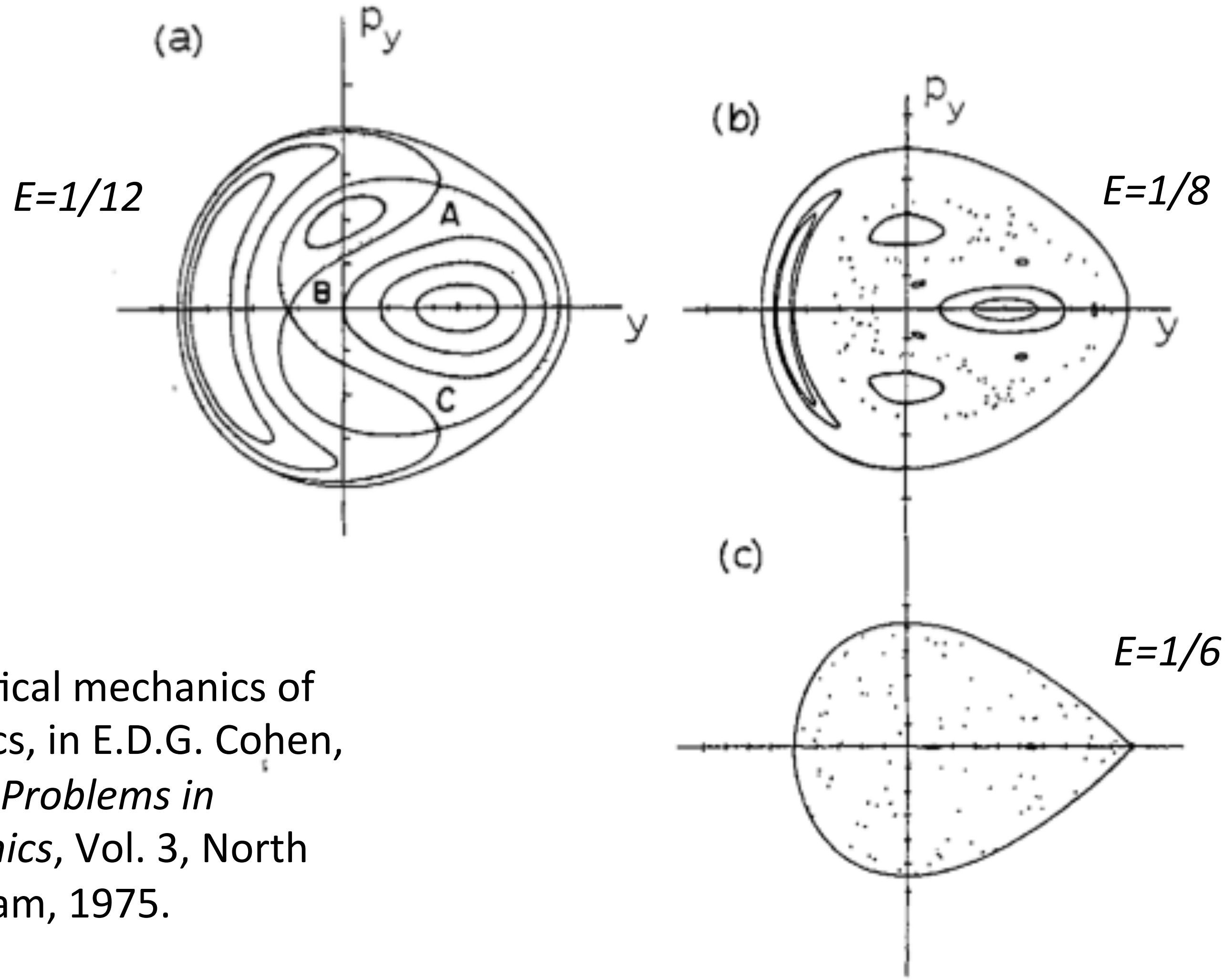


J. Ford, The statistical mechanics of analytical dynamics, in E.D.G. Cohen, Ed., *Fundamental Problems in Statistical Mechanics*, Vol. 3, North Holland, Amsterdam, 1975.

# You Tube

- http://www.youtube.com/watch?v=rEoUMKxbuvA

# Another example: spin coupled to a harmonic oscillator (Dicke model)

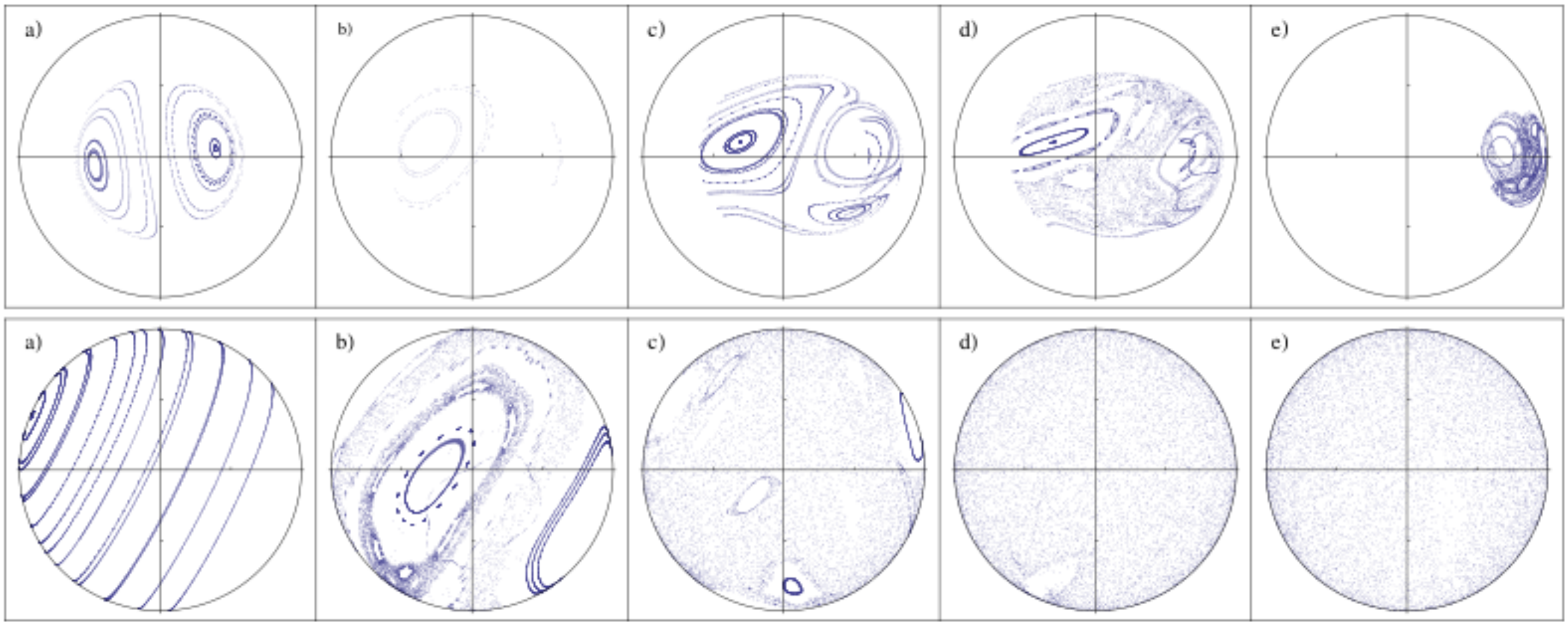


FIG. 1 (color online). Poincaré sections generated by monitoring the projection $(l_x, l_y)$ of $l$ in the southern hemisphere at fixed values of the phase $\psi$. For each parameter value, $g/g_c$, nine trajectories of different on-shell initial conditions are sampled. Upper row: Energy $\Delta\epsilon \simeq 0.2|\epsilon_0|$ above the ground state and values $g/g_c$ (a) 0.2, (b) 0.7, (c) 0.9, (d) 1.01, (e) 1.5. Lower row: Energy $\Delta\epsilon \simeq 20|\epsilon_0|$.

$$\hat{H} = \hbar\left\{\omega_0 \hat{J}_z + \omega \hat{a}^\dagger \hat{a} + g\sqrt{\frac{2}{j}}(\hat{a}+\hat{a}^\dagger)\hat{J}_x\right\}$$

Spin j coupled to a harmonic oscillator

Altland and Haake, Phys. Rev. Lett. **108**, 073601 (2012).

# Henon map (1969)

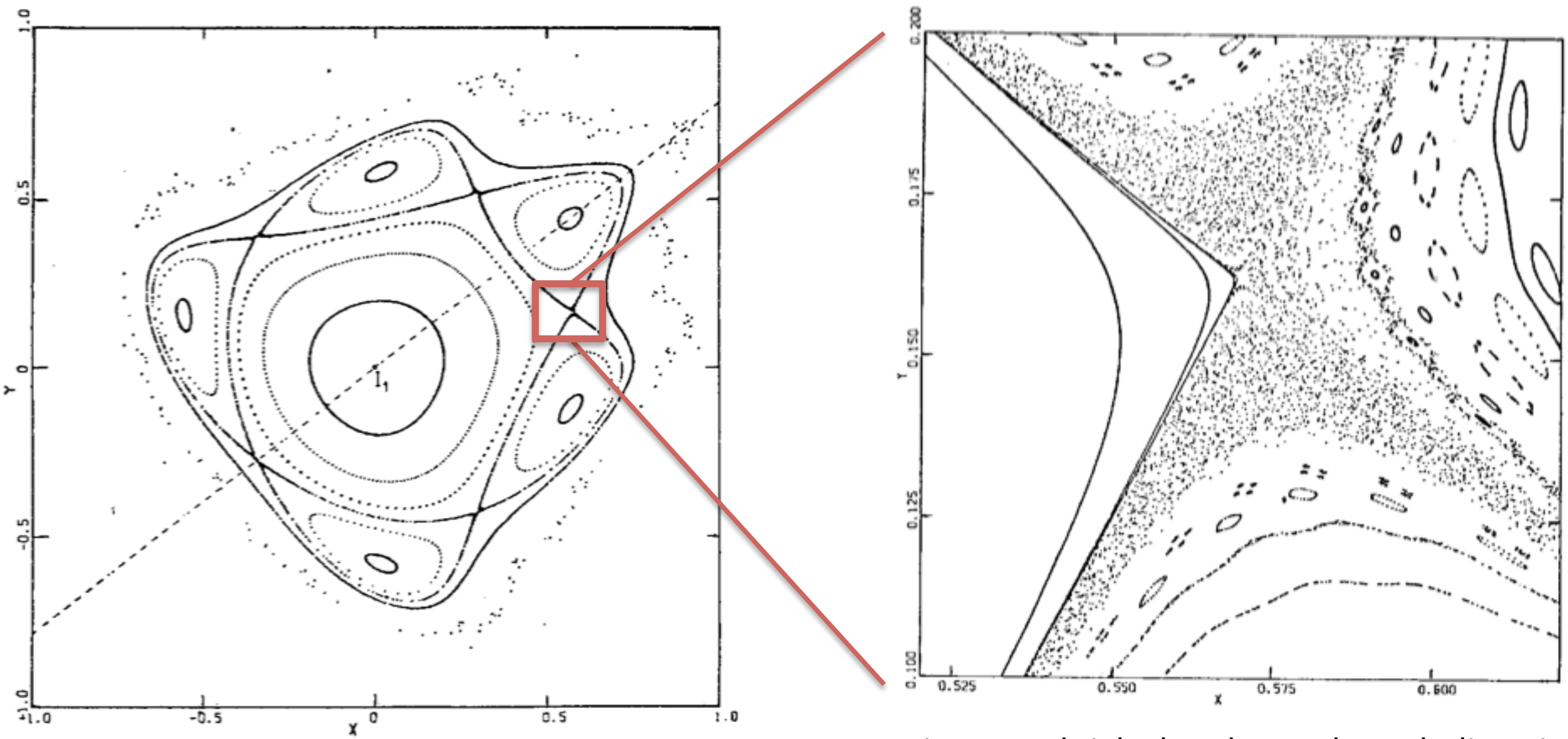


α=0.2114

Zoom-in around right-hand-most hyperbolic point

*T₁*:

$$x_{i+1/2} = x_i$$
$$y_{i+1/2} = y_i - x_i^2$$

$T_2$:

$$x_{i+1} = x_{i+1/2}\cos\alpha - y_{i+1/2}\sin\alpha$$
$$y_{i+1} = x_{i+1/2}\sin\alpha + y_{i+1/2}\cos\alpha$$

$T=T_1T_2$

# Mandelbrot set (two dimensional fractal shape)

Map in complex plane: $z_{n+1} = z_n^2 + c$

Starts from initial point: $z_0 = 0$

The complex numbers $C$ for which $|z_n|$ remains a finite number as $n$ tends to infinity make up the Mandelbrot set (the black points in the picture).

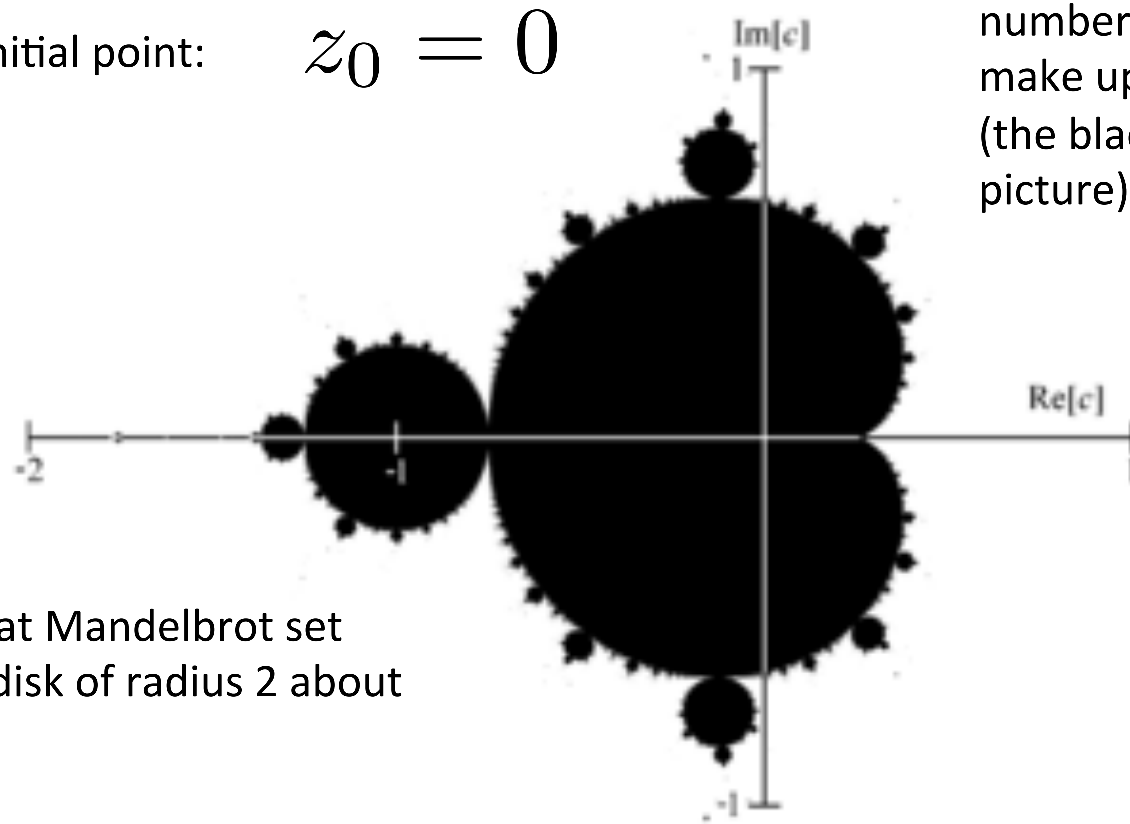


Can prove that Mandelbrot set lies within a disk of radius 2 about the origin.

Example 1: $C$=1 gives:
0,1,2,5,26… tends to infinity

Example 2: $C$=i gives:
0,i,-1+i,-2i,-i,-1+i,… remains bounded

# Self-similarity

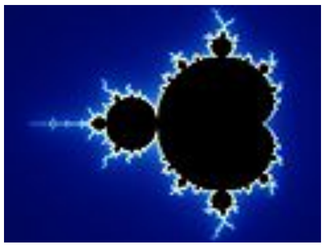

Gap between head and body called the "seahorse valley"

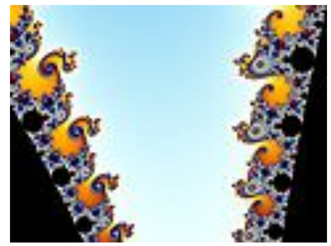

Double spiral on the left, seahorses on the right.

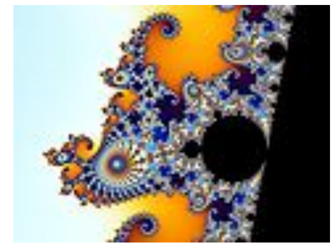

An upside down seahorse

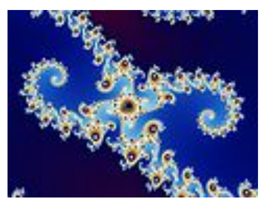

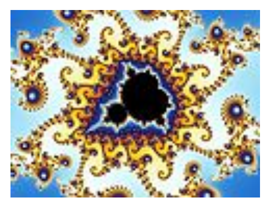

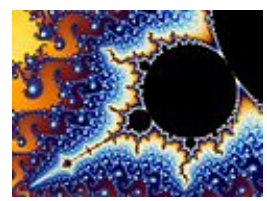

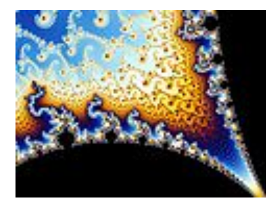

# The logistic map

Logistic: $$x_{n+1} = f(x_n)$$

where $$f(x) = 4\lambda x(1-x)$$

Mandelbrot: $$z_{n+1} = z_n^2 + c$$

There is a correspondence between the two maps along the real line if we put:

$$c = \frac{\lambda}{2}(1 - \frac{\lambda}{2})$$

# Motivation for the logistic map

Biological model for population growth:

$$x_{n+1} = rx_n - sx_n^2$$

*r:* rate constant quantifying ability of population to reproduce
*s:* parameter quantifying the effect of over crowding

Cf. logistic differential equation: $\dot{x} = kx - \sigma x^2$

which has solution: $x(t) = \dfrac{kx_0}{\sigma x_0 + (k - \sigma x_0)\exp(-kt)} \quad \text{for} \quad x_0 > 0$

Logistic map: $x_{n+1} = 4\lambda x_n - 4\lambda x_n^2$

# How the logistic map works

$$\boxed{\begin{aligned} x_{n+1} &= f(x_n) \\ f(x) &= 4\lambda x(1-x) \end{aligned}}$$

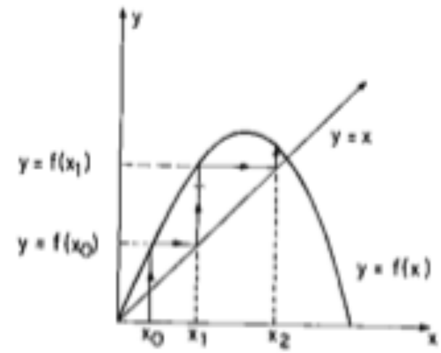


(a)

Fixed points:

$$\boxed{x^\star = 0 \quad \text{and} \quad x^\star = 1 - (4\lambda)^{-1}}$$

i.e. solutions of $\quad x^\star = 4\lambda x^\star(1 - x^\star)$

Stability of fixed points:

consider $x_n = x^\star + \epsilon_n$

$$x_{n+1} = f(x^\star + \epsilon_n) \approx f(x^\star) + \epsilon_n f'(x^\star)$$
$$= x^\star + \epsilon_n f'(x^\star)$$

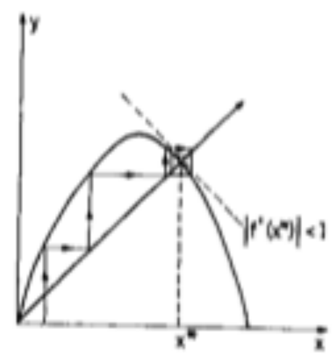


(b)

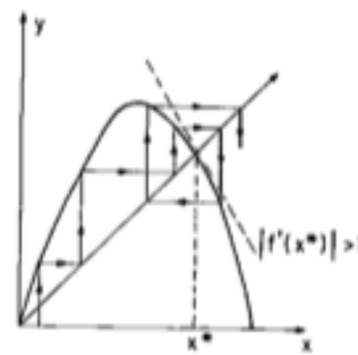


(c)

but $\quad x_{n+1} = x^\star + \epsilon_{n+1} \qquad$ so $\quad \dfrac{\epsilon_{n+1}}{\epsilon_n} = f'(x^\star)$ $\Rightarrow$ converges if $\quad |f'(x^\star)| < 1$

# Period doubling

For λ<1/4 all iterates converge to $x^{\star}$=0.
For 1/4<λ<3/4 all iterates converge to $x^{\star}$=1-1/4λ.

For λ>3/4 the latter fixed point becomes unstable (at λ=3/4 $f'(x^{\star})=-1$). Actually, it bifurcates into two stable fixed points. These are fixed points of

$$f^2 = f(f(x))$$

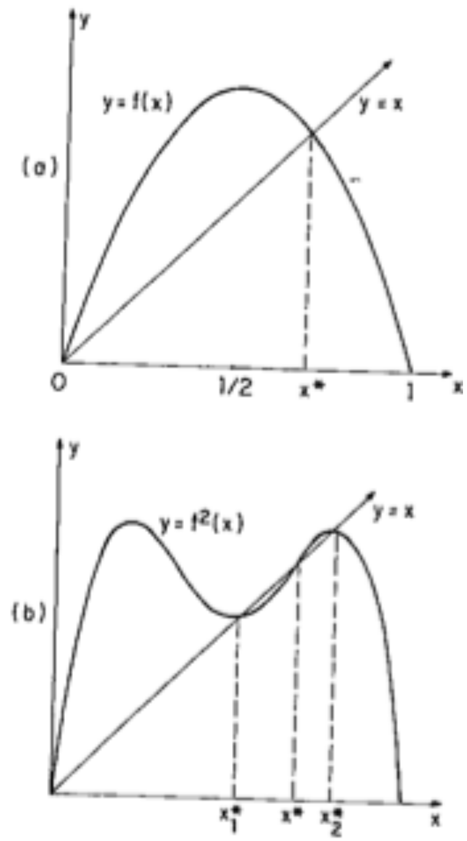


For λ> ¾ , $x^{\star}_1$ and $x^{\star}_2$ are the fixed points of $f^2$.
They are not fixed points of $f$, but are mapped into each other under $f$, forming a 2-cycle:

$$x_1^{\star} = f(x_2^{\star}) \quad \text{and} \quad x_2^{\star} = f(x_1^{\star})$$

An initial point eventually settles into the sequence:

$$x_1^{\star}, x_2^{\star}, x_1^{\star}, x_2^{\star}, x_1^{\star}, x_2^{\star}, \ldots$$

# 4-cycle

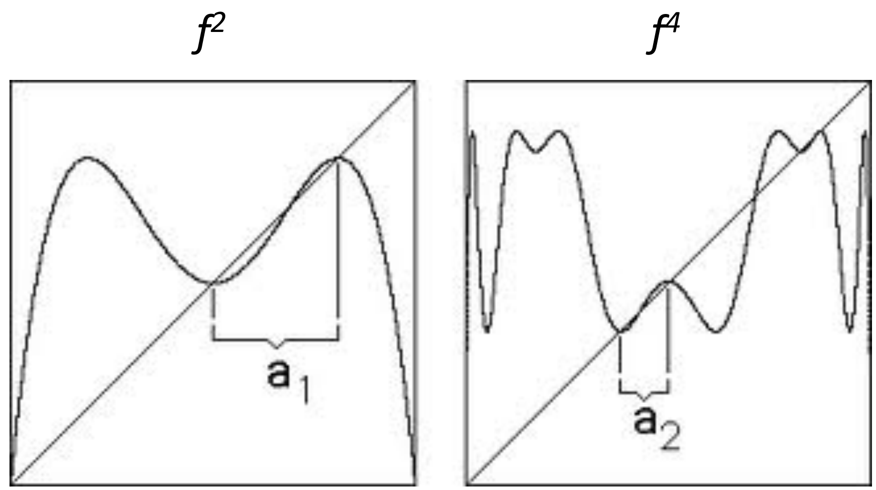

# Stability of n-cycles

Consider $f^2$: define $x_2 = f^2(x_0) = f(x_1)$ where $x_1 = f(x_0)$

Chain rule:

$$\left.\frac{d}{dx}f^2(x)\right|_{x=x_0} = \left.\frac{d}{dx}f(x_1)\right|_{x=x_0} = \left.\frac{d}{dx_1}f(x_1)\frac{dx_1}{dx}\right|_{x=x_0} = \left.\frac{d}{dx_1}f(x_1)\frac{d}{dx}f(x)\right|_{x=x_0}$$

Can easily generalize to:

$$\left.\frac{d}{dx}f^n(x)\right|_{x=x_0} = f'(x_0)f'(x_1)f'(x_2)\dots f'(x_{n-1})$$

If λ<¾ then for the fixed point $x^\star=x_0$, clearly $x_2=x_1=x^\star$ and hence $f^{2\prime}(x^\star) = f'(x^\star)f'(x^\star) = (f'(x^\star))^2$
Thus if $|f'(x)| < 1$ then $|f^{2\prime}(x)| < 1$. So if $x^\star$ is a stable point of *f*, it is also a stable point of $f^2$.

If λ>¾ then $x_1^\star = f(x_2^\star)$ and $x_2^\star = f(x_1^\star)$ and neither of these points are fixed points of *f.*
However, the slope of $f^2$ at $x_1^\star$ and $x_2^\star$ are the same, i.e.

$$f^{2\prime}(x_2^\star) = f'(x_1^\star)f'(x_2^\star) \quad \text{and} \quad f^{2\prime}(x_1^\star) = f'(x_2^\star)f'(x_1^\star)$$

Thus, $x_1^\star$ and $x_2^\star$ are simultaneously stable for λ>¾ and become simultaneously unstable at some larger value of λ.

# Period doubling bifurcations of the logistic map

- For small λ all iterates (providing $x_0 \neq 0$) converge onto a single limit point. The behaviour persists until λ>0.75.
- For larger λ the single limit point bifurcates into a pair of fixed points (period-2 limit cycle).
- Increasing λ further the period-2 limit cycle bifurcates into a period-4 cycle, which subsequently bifurcates into a period-8 cycle, and so on.
- The λ values at which the bifurcations occur ($\lambda_1$, $\lambda_2$, …) become ever closer and converge geometrically to a critical value $\lambda_\infty$ (about 0.892) where the orbit becomes aperiodic (has infinite period).
- Beyond $\lambda_\infty$ both chaotic orbits and odd period limit cycles occur.
- At λ=1 the motion is formally ergodic on the unit interval (0,1); beyond λ=1 all orbits escape to infinity.

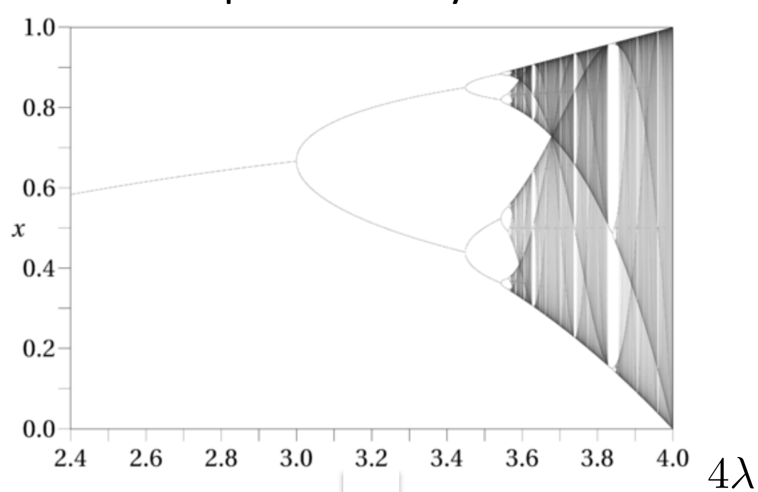


$$x_{n+1} = 4\lambda x_n(1 - x_n)$$

$$0 < x < 1$$

# "Period 3 implies chaos"★

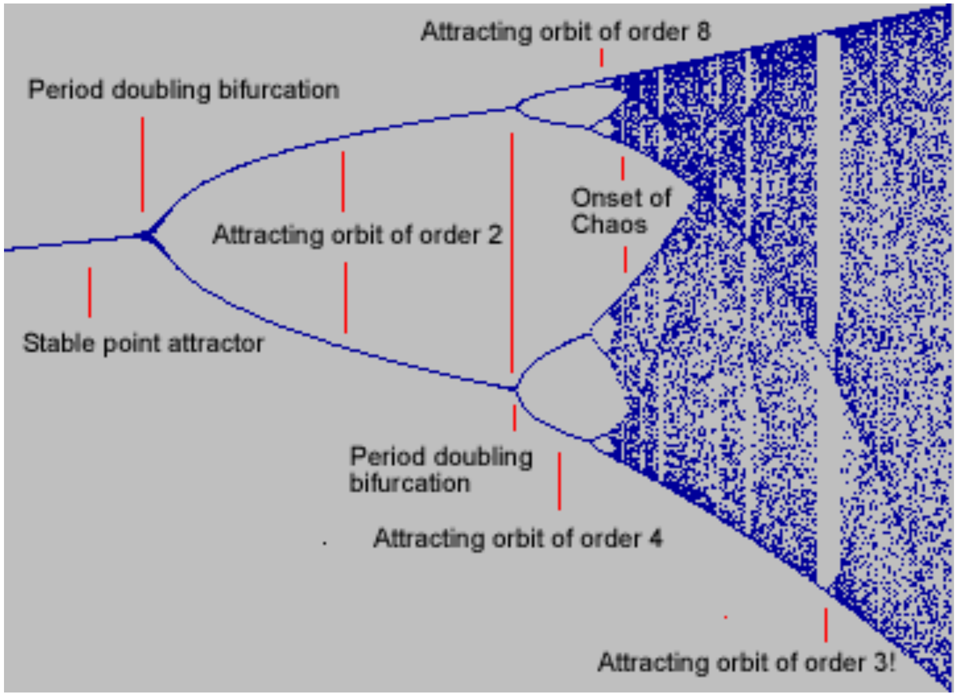


The appearance of odd-period cycles seems to be intimately connected to the appearance of chaos.

★ Li and Yorke, *Period three implies chaos,* Am. Math. Monthly **82**, 985 (1975).

# Feigenbaum number

In 1978 Feigenbaum noticed a geometric convergence of the period doubling sequence:

$$\lambda_\infty - \lambda_n \propto \frac{1}{\delta^n}$$

e.g. can define $$\delta_n = \frac{\lambda_{n+1} - \lambda_n}{\lambda_{n+2} - \lambda_{n+1}}$$

As *n* tend to infinity $$\delta \to 4.6692016$$

Remarkably, other nonlinear maps (Henon map, Lorenz model, small mode truncations of the Navier-Stokes equations) have this same convergence rate. Thus, δ is a universal number, at least for a certain class of map.

# Rayleigh-Benard convection

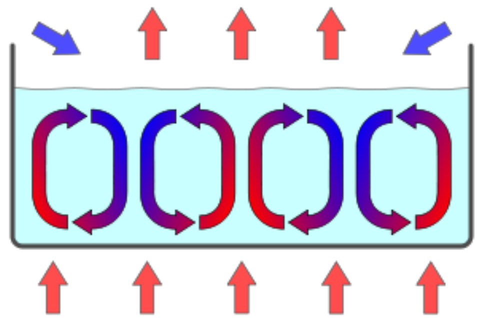

Rayleigh-Benard convection for mercury in a magnetic field shows at least four period doublings with a universal scaling that agrees with Feigenbaum's number to within 5% (Libchaber et al, *Two Parameter study of routes to chaos,* Physica **7D**, 69 (1983).